







Genetic and Antigenic Characterization of an Expanding H3 Influenza A Virus Clade in U.S. Swine Visualized by Nextstrain

Megan N. Neveau,^{a,b}  Michael A. Zeller,^a Bryan S. Kaplan,^c Carine K. Souza,^c  Phillip C. Gauger,^a  Amy L. Vincent,^c  Tavis K. Anderson^c

^aDepartment of Veterinary Diagnostic and Production Animal Medicine, College of Veterinary Medicine, Iowa State University, Ames, Iowa, USA

^bBioinformatics and Computational Biology Program, Iowa State University, Ames, Iowa, USA

^cVirus and Prion Research Unit, National Animal Disease Center, USDA-ARS, Ames, Iowa, USA

ABSTRACT Defining factors that influence spatial and temporal patterns of influenza A virus (IAV) is essential to inform vaccine strain selection and strategies to reduce the spread of potentially zoonotic swine-origin IAV. The relative frequency of detection of the H3 phylogenetic clade 1990.4.a (colloquially known as C-IVA) in U.S. swine declined to 7% in 2017 but increased to 32% in 2019. We conducted phylogenetic and phenotypic analyses to determine putative mechanisms associated with increased detection. We created an implementation of Nextstrain to visualize the emergence, spatial spread, and genetic evolution of H3 IAV in swine, identifying two C-IVA clades that emerged in 2017 and cocirculated in multiple U.S. states. Phylodynamic analysis of the hemagglutinin (HA) gene documented low relative genetic diversity from 2017 to 2019, suggesting clonal expansion. The major H3 C-IVA clade contained an N156H amino acid substitution, but hemagglutination inhibition (HI) assays demonstrated no significant antigenic drift. The minor HA clade was paired with the neuraminidase (NA) clade N2-2002B prior to 2016 but acquired and maintained an N2-2002A in 2016, resulting in a loss of antigenic cross-reactivity between N2-2002B- and -2002A-containing H3N2 strains. The major C-IVA clade viruses acquired a nucleoprotein (NP) of the H1N1pdm09 lineage through reassortment in the replacement of the North American swine-lineage NP. Instead of genetic or antigenic diversity within the C-IVA HA, our data suggest that population immunity to H3 2010.1 along with the antigenic diversity of the NA and the acquisition of the H1N1pdm09 NP gene likely explain the reemergence and transmission of C-IVA H3N2 in swine.

IMPORTANCE Genetically distinct clades of influenza A virus (IAV) in swine undermine efforts to control the disease. Swine producers commonly use vaccines, and vaccine strains are selected by identifying the most common hemagglutinin (HA) gene from viruses detected in a farm or a region. In 2019, we identified an increase in the detection frequency of an H3 phylogenetic clade, C-IVA, which was previously circulating at much lower levels in U.S. swine. Our study identified genetic and antigenic factors contributing to its resurgence by linking comprehensive phylodynamic analyses with empirical wet-lab experiments and visualized these evolutionary analyses in a Nextstrain implementation. The contemporary C-IVA HA genes did not demonstrate an increase in genetic diversity or significant antigenic changes. N2 genes did demonstrate antigenic diversity, and the expanding C-IVA clade acquired a nucleoprotein (NP) gene segment via reassortment. Virus phenotype and vaccination targeting prior dominant HA clades likely contributed to the clade's success.

KEYWORDS influenza A virus, H3N2, swine, reassortment, surveillance, vaccines, Nextstrain, genomic epidemiology, influenza

Editor Anice C. Lowen, Emory University School of Medicine

This is a work of the U.S. Government and is not subject to copyright protection in the United States. Foreign copyrights may apply.

Address correspondence to Tavis K. Anderson, tavis.anderson@usda.gov.

The authors declare no conflict of interest.

Received 17 December 2021

Accepted 8 April 2022

Published 9 May 2022

Influenza A virus (IAV) is an economically important pathogen of swine that has the ability to evolve and evade the host immune response, which presents a challenge to current control strategies. The negative-sense, single-stranded RNA genome consists of eight noncontiguous gene segments that are known to encode between 10 and 17 proteins (1–3). The segmented genome structure creates the opportunity for reassortment when two or more IAV strains concurrently infect the same host, resulting in novel gene combinations and increased diversity at the genomic level (4, 5). IAV can also rapidly accumulate mutations due to errors introduced by viral polymerase (6). Swine have both α 2,6- and α 2,3-Gal-linked sialic acid on the surface of their respiratory epithelial cells; therefore, in addition to swine-to-swine transmission, they have the potential for infection from human- and avian-origin IAVs (7, 8). Consequently, observed IAV diversity in swine is increased by the transmission, occasional establishment, and evolution of avian and human IAVs in swine populations.

The genetic diversity of IAV translates to a similarly large breadth of antigenic diversity in the hemagglutinin (HA) and neuraminidase (NA) proteins. The accumulation of amino acid substitutions from polymerase mutation in the surface glycoproteins often results in changes in the antigenic phenotype of IAV (9, 10). For the H3 subtype, a small number of amino acid residues have a disproportionate effect on antigenic phenotype in both humans and swine (11–13). Six of these amino acid positions (145, 155, 156, 158, 159, and 189 [H3 mature peptide numbering {14}]) are referred to as the H3 antigenic motif in swine (15). These 6 residues are located on the globular head of the HA protein and are adjacent to the receptor binding site. There may be constraints on substitution flexibility at these positions due to the necessary conservation of receptor binding functionality, as shown for position 145 (13). Minimal genetic change may result in significant antigenic change, reducing the efficacy of current IAV vaccines against clinical disease and transmission in swine (16). Vaccination with whole inactivated virus (WIV) with an oil-in-water adjuvant is common in swine in the United States. However, WIVs are most efficacious when the vaccine and challenge strains are closely related (17, 18). Thus, an important utility of IAV surveillance and sequence data in swine populations is to inform vaccine strain selection.

In 1998, investigations into severe respiratory disease in swine in the United States revealed the introduction of the H3N2 subtype of IAV into swine. The H3N2 viruses that persisted had triple-reassortant internal genes (TRIGs) with HA, NA, and PB1 gene segments derived from human seasonal H3N2; PB2 and PA gene segments from avian IAV; and nucleoprotein (NP), M, and NS gene segments from classical swine H1N1 (19–21). The HA gene from this introduction established the colloquially named H3 cluster IV (C-IV) in the United States (named the 1990.4 lineage in global H3 nomenclature [21]). The C-IV HA continued to circulate in the United States and evolved into genetically distinct clades A through F (22). C-IV clade A (C-IVA) began to increase in detection frequency beginning in 2010 and was the predominant H3 clade in U.S. swine until 2016 when it was surpassed by H3 2010.1, a more recent human seasonal incursion that subsequently became established as a swine lineage (21, 23, 24). In recognition of the animal and public health relevance of IAV in swine, the U.S. Department of Agriculture (USDA) implemented a surveillance system beginning in 2010 (25). The system allows producers to voluntarily and anonymously submit samples collected from swine exhibiting influenza-like illness to regional veterinary diagnostic laboratories for diagnostics and sequencing of the HA and NA genes. The surveillance system has resulted in the collection of 9,391 IAV isolates and the publication of 9,040 HA sequences as of 30 September 2021 (26). The data collected within the system have been applied to monitor spatial and temporal trends in the genetic and antigenic diversity of IAV in swine across the sampled areas of the United States (11, 27).

In this study, we used the USDA IAV-in-swine surveillance data set, supplemented with other publicly available sequence data, to describe a resurgence in C-IVA sequence detections in 2019 as well as a relative decrease in the detection of H3 2010.1. We quantified genetic and antigenic characteristics associated with the

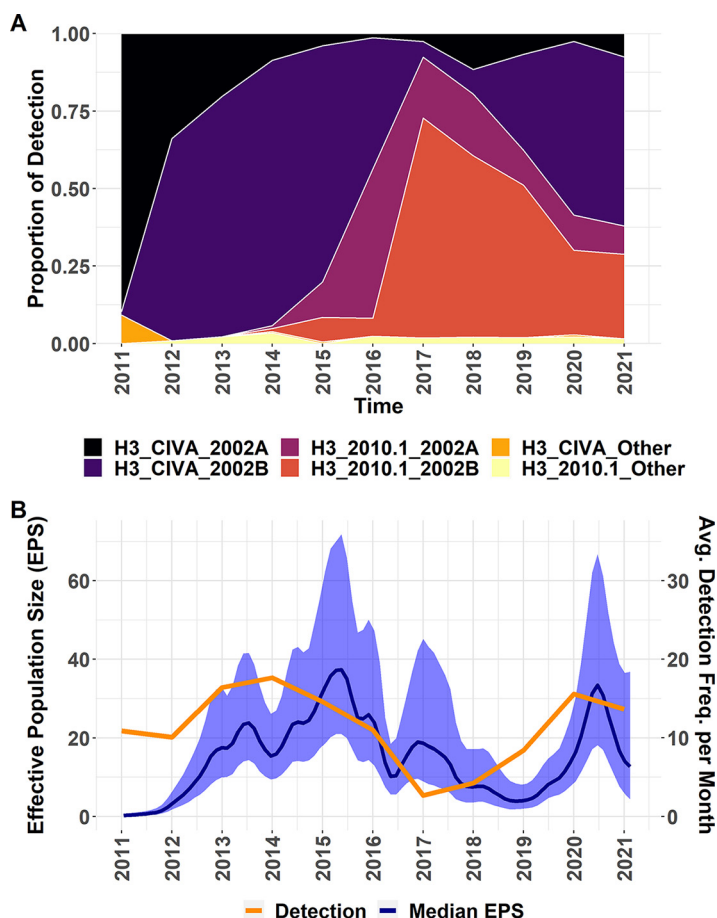


FIG 1 Relative C-IVA and 2010.1 HA-NA pair detection frequency and relative C-IVA genetic diversity from 2011 to 2021. (A) Proportional yearly detection frequency of H3 clades C-IVA and 2010.1 with the corresponding NA genetic clade from public data. In the key, the HA clade is followed by the NA clade. “Other” includes NA genes from the N2-1998 clade and one-off human-to-swine transmission events. (B) EPS and average detection frequency per month of C-IVA viruses. EPS estimates relative genetic diversity within the HA genes of the C-IVA clade. Blue shading is the 95% highest posterior density (HPD) interval.

increased detection frequency of the C-IVA clade. Concurrently, we adapted the Nextstrain platform (28) to IAV in swine to provide near-real-time phylogenetic visualization of surveillance data for the H3 subtype. Collectively, these analyses provide insight into the factors contributing to the expansion of swine IAV clades and improve our ability to predict mechanisms that allow IAV to evade current control measures in swine populations.

RESULTS

Increased detection frequency followed by increased relative genetic diversity of H3 clade IVA. From 2011 to 2015, the C-IVA genetic clade was detected more frequently in U.S. swine than the 2010.1 genetic clade (Fig. 1A). Between 2011 and 2014, the C-IVA clade paired with an N2-2002B gene was the primary HA-NA pairing detected among H3N2 viruses, while the C-IVA clade paired with an N2-2002A gene had a decreased detection frequency. From 2015 to 2017, the C-IVA clade paired with an N2-2002B gene decreased in detection frequency, and detections of the 2010.1 HA clade paired with N2-2002A and -2002B genes increased from less than 20% to more than 90%. After 2017, the majority of 2010.1 (69%) viruses detected were paired with an N2-2002B. In 2018, the H3 clade frequency patterns abruptly changed again, with C-IVA at 39% of H3 HA genes. In 2019, the C-IVA HA genes were detected at 75%, and in 2020, the C-IVA HA genes represented more than 80% of the H3 genes in

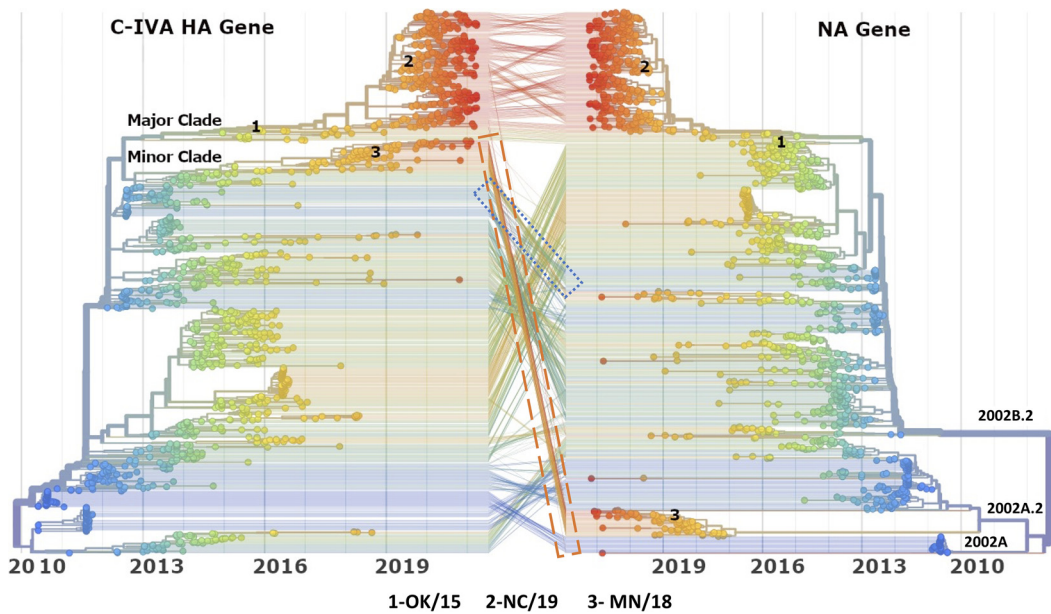


FIG 2 Tanglegram of the corresponding C-IVA HA and NA gene time-scaled phylogenetic trees with sequences from 2010 to March 2021. The major and minor contemporary C-IVA clades are labeled on the HA tree. N2 genetic clades are labeled on the NA tree. The three contemporary C-IVA strains used for antigenic analysis are also labeled on both trees (1, A/swine/Oklahoma/A01770191/2015 [OK/15]; 2, A/swine/North Carolina/A02245294/2019 [NC/19]; 3, A/swine/Minnesota/A02266068/2018 [MN/18]). Lines between the two trees indicate HA-NA pairing. Tree branches and leaves are colored on a blue-to-red gradient by the yearly progression of time in accordance with the x axis. The blue dotted line indicates the pairing of the minor clade with N2-2002B prior to reassortment, and the orange dashed line indicates reassortment of the minor clade with N2-2002A. The Nextstrain platform can be used to visualize the tanglegram in finer detail at <https://flu-crew.org/>.

surveillance. The patterns in the detection of the C-IVA and 2010.1 H3 clades in the first 3 months of 2021 remained similar to those in 2020. Throughout this time period, the detection of H1 to H3 genes was relatively stable and concordant with previous reports of approximately 70% H1 genetic clades and 30% H3 genetic clades (see Fig. S1 in the supplemental material) (27).

To investigate the C-IVA expansion, we measured the median posterior rate of nucleotide substitution for the C-IVA clade by Bayesian analysis to be 4.265×10^{-3} (95% highest posterior density [HPD], 3.956×10^{-3} , 4.589×10^{-3}). The relative genetic diversity of the HA gene was estimated by a Bayesian demographic reconstruction and demonstrated an almost linear increase in the median effective population size (EPS) for C-IVA genes from 2011 to 2015 but a decrease from 2015 to 2019 (Fig. 1B). Despite minimal relative genetic diversity in 2018 and 2019, the detection frequency began to increase. The increase in the relative genetic diversity in 2020 lagged behind the increase in the detection frequency. The trends in relative genetic diversity are supported by the topology of a maximum likelihood phylogeny (Fig. S2), with external branches that are shorter than branches on the interior of the tree; i.e., the topology of the phylogeny is balanced in the major clade of C-IVA detected from 2019 to the present (see the HA gene tree in Fig. 2). The equal and undirected propagation of leaves along the branches suggests that selection is not acting on the HA gene at the time of this study, as HA under selection would appear as a “ladder-like” topology across the entire gene tree.

Two cocirculating clades with onward transmission after 2018. The HA tree (Fig. 2) shows at least 8 cocirculating C-IVA genetic clades that corresponded to high levels of relative genetic diversity in 2013 and 2015 (Fig. 1B). These clades contained detections from 21 different states, primarily in the Midwest. In 2017 and 2018, the C-IVA HA gene was detected across 12 states, mostly in the Midwest and Southwest. After 2018, only two distinct genetic clades of C-IVA were apparent: a major clade representing 245 detections

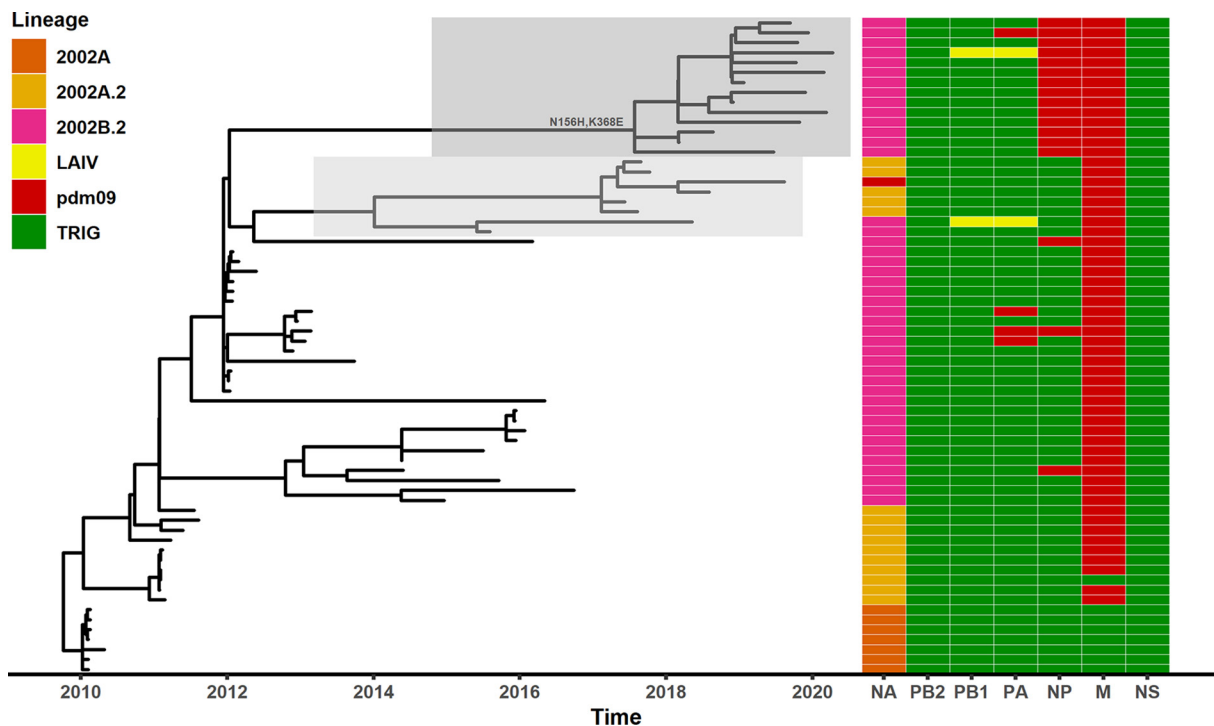


FIG 3 C-IVA HA time-scaled tree with genome constellation. The corresponding NA and internal gene (PB2, PB1, PA, NP, M, and NS) lineages of each tip are indicated by the color-coded rectangles on the right. The major contemporary C-IVA clade is boxed in dark gray on the tree, and the minor contemporary C-IVA clade is boxed in light gray on the tree. The two substitutions defining the initial expansion of the major clade (N156H and K368E) are annotated on the tree. LAIV, live attenuated influenza vaccine; TRIG, triple-reassortant internal gene.

(71 in 2019 and 174 in 2020) and a minor clade representing 24 detections (19 in 2019 and 6 in 2020). The major clade viruses were first detected in the Southwest region (Texas, Oklahoma, and Kansas) in 2017 and 2018 but were detected in the major pork-producing states of the Midwest by January 2019. By late 2019, major clade viruses were also detected in North Carolina and some less-hog-dense states such as Michigan and Pennsylvania. Although there was broad geographic representation, 56% of the detections of this clade were in Iowa and Indiana. The minor clade was initially detected in the Midwest, with only 5 detections outside this region from 2018 to the present.

Reassortment with the H3 IVA and novel NA and NP gene segment pairings. The HA gene segments of the major C-IVA clade paired consistently with N2 clade 2002B.2 gene segments, matching the topology of the congruent NA phylogenetic tree (Fig. 2). The minor clade HA genes were paired with N2-2002B.2 from mid-2012 to 2016. In 2016 (95% confidence interval [CI], 5 June 2016, 8 February 2017), the minor clade showed evidence of reassortment with a genetically distinct N2-2002A.2 clade that no other C-IVA HA gene segment was paired with in the past decade. To identify the donor of the N2-2002A.2 gene to the minor C-IVA clade, a phylodynamic analysis was conducted and determined that the likely donor was an H1 beta virus (Fig. S3). To observe patterns in the available genomes of the IVA H3N2 strains, the lineages of the remaining six gene segments were annotated onto the HA tree (Fig. 3).

Shortly after the 2009 H1N1 pandemic, North American swine IAV acquired the M gene from the H1N1pdm09 (pdm) lineage but retained a nucleoprotein (NP) gene segment from the triple-reassortant H3N2 (TRIG) lineage. The major clade showed evidence of reassortment with an NP from the pdm lineage in 2017. A phylodynamic analysis of NP genes, including human seasonal H1 pdm NP, revealed that the most likely common ancestor of the C-IVA pdm lineage NP in the major clade was other endemic swine H3 viruses (2010.1) that had acquired the pdm NP following reassortment with swine H1 delta1 viruses that had also acquired the pdm NP via reassortment in approximately 2009 (Fig. S4). All available whole-genome sequences (*n* = 58) from the major clade after

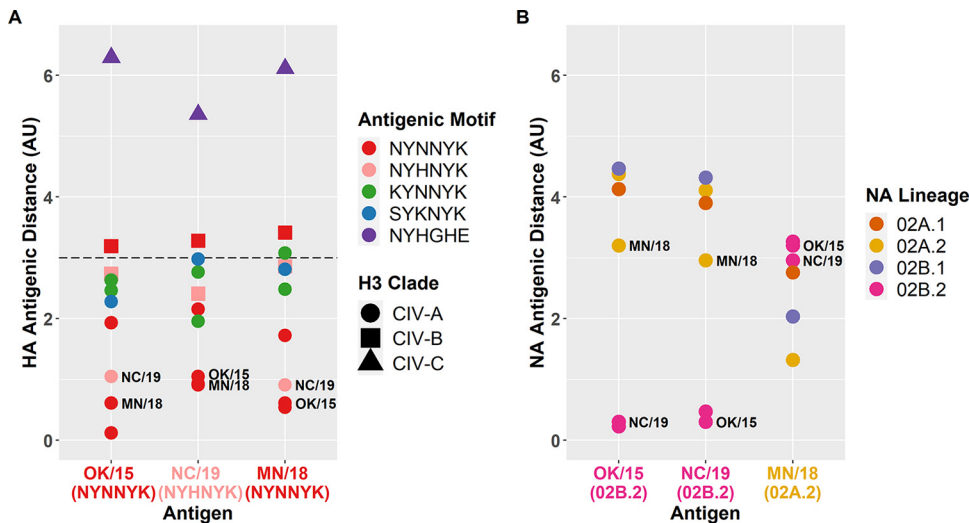


FIG 4 HA and NA antigenic distances. (A) HA antigenic distance between three contemporary C-IVA test antigens and relevant H3 reference antigens. Distances are computed by merging the raw HI results from the assay described in this experiment with results from previous HI assays in ACMACS. Points are colored by H3 antigenic motif, and their shape corresponds to their H3 clade classification. The three test antigens on the x axis are colored by H3 antigenic motif. Significant HA antigenic drift is defined as an antigenic distance of at least 3 AU and is denoted by the black dashed line. (B) NA antigenic distance between three contemporary C-IVA test antigens and antigens from four N2-2002 lineages. Distances are computed by merging the raw NI results from the assay described in this experiment with results from previous NI assays in ACMACS. Points are colored by NA lineage. The three test antigens on the x axis are also colored by NA lineage. The test antigens OK/15, NC/10, and MN/18, are labeled with black text in both panels.

September 2018 retained a pdm lineage NP, with additional reassortment events from different donor H1 and H3 viruses occurring during this time. There was no evidence of replacement of the TRIG lineage in the PB2, PB1, PA, or NS gene segments.

N156H antigenic motif substitution. The time-scaled tree annotated with amino acid substitutions created with Nextstrain showed two amino acid substitutions associated with the expansion of the major clade, N156H and K368E, dating to November 2016 (95% CI, 4 June 2016, 18 May 2017) (Fig. 3). Position 156 was identified in the previously characterized antigenic motif (11, 12, 15). Thirteen other amino acid substitutions were detected in H3 genes in the major clade after December 2016 but with no consistent pattern. Five of the 13 occurred in antigenic regions of HA1 (N96S, S146G, N158D, I214V, and V323I [H3 mature peptide numbering]) (29).

Antigenic diversity of HA. Contemporary strains were selected to represent three groups of C-IVA for antigenic assessment of the HA (Table S1): the major clade prior to the N156H substitution (A/swine/Oklahoma/A01770191/2015 [OK/15]) (annotation 1 in Fig. 2) with a motif of NYNNYK, the major clade following the N156H substitution (A/swine/North Carolina/A02245294/2019 [NC/19]) (annotation 2 in Fig. 2) with a motif of NYHNYK, and the minor clade (A/swine/Minnesota/A02266068/2018 [MN/18]) (annotation 3 in Fig. 2) with a motif of NYNNYK. Significant antigenic drift is defined by an 8-fold loss in hemagglutination inhibition (HI) cross-reactivity, which corresponds to 3 antigenic units (AU) between viruses in an antigenic map. The three contemporary C-IVA representative strains were within 2 AU of each other and within 3 AU of the other C-IVA strains tested (Fig. 4A). Two reference antigens from a different genetic clade, C-IVB, were near the 3-AU significance cutoff. The C-IVB strain representing the NYHNYK antigenic motif was closer to all three tested C-IVA viruses, particularly NC/19, which had the same NYHNYK antigenic motif, than the C-IVB strain representing the NYNNYK antigenic motif. The representative strain of C-IVC showed a significant antigenic distance of over 5 AU from the C-IVA strains.

Neuraminidase inhibition and diversity determined by an enzyme-linked lectin assay (ELLA). The neuraminidase-inhibiting (NI) titers of the same three HI test strains were assessed against reference antisera of swine N2 clades (Table S2): the OK/15

and NC/19 strains had an N2-2002B.2 gene, and the minor clade representative MN/18 had an N2-2002A.2 gene. These new NI titer data were combined with data from previous experiments by Kaplan et al. (30), and antigenic distances were extracted. There were differences in NI antigenic phenotype within the N2-2002 lineage, which was further divided into 2002A.1, 2002A.2, 2002B.1, and 2002B.2 (30, 31). In particular, the minor clade MN/18 virus with the 2002A.2 lineage had an antigenic distance of 3 AU from the 2002B.2 lineage viruses, including the major clade NC/19 virus (Fig. 4B). Despite being isolated 4 years apart, the 2002B.2 lineage viruses retained NI antigenic properties and were within 0.5 AU of each other.

DISCUSSION

This study investigated the recent increase in the detection of H3 C-IVA viruses in U.S. swine and how circulating H3 diversity within swine populations could help explain genetic clade turnover and dominance dynamics. The H3 2010.1 clade that emerged in 2012 began to supplant the C-IVA clade in 2016 (Fig. 1A). There was limited serological cross-reactivity between 2010.1 and C-IVA swine H3N2 viruses (24). Animals in the population in 2016 were more likely to have natural immunity against 2010.1 viruses, while animals with natural immunity against C-IVA viruses gradually decreased.

Vaccine immunity likely plays a significant role in the dynamics of HA clades detected in the United States. There is only one fully licensed commercial swine IAV vaccine, and this does not contain the 2010.1 antigen; instead, it has an H3 C-IVA antigen, an H3 C-IVB antigen, and two H1 antigens (H1N1 gamma and H1N2 delta1) (32). Consequently, instead of a commercial product, many swine in production systems were likely vaccinated against the 2010.1 clade of viruses with custom or autogenous vaccines following its emergence and dominance over C-IVA (16, 33). In 2012, 60% of producers of large breeding herds reported the use of an influenza vaccine, and 47% of those were using autogenous vaccines rather than a fully licensed product (34). Thus, waning immunity against C-IVA viruses due to decreased natural immunity and the increased use of vaccines containing 2010.1 viruses could have provided an advantage to the C-IVA viruses. This is supported by the balanced shape of the HA phylogeny of the major clade after 2019, which suggests an absence of immune- or vaccine-driven selection within the C-IVA major clade (Fig. 2 and 3).

Although the number of C-IVA detections increased since 2018, the relative genetic diversity within the clade did not increase until mid-2020. The 2018–2019 clonal expansion of C-IVA with low diversity suggests that a selective sweep occurred in the population. Sweep-related changes have been identified in human seasonal H3N2 IAV and are most often detected at amino acid sites located on the HA (35, 36). In 2019, the relative genetic diversity began to rise, likely as the result of the success, spread, and subsequent diversification of the virus. It is important to note that detection frequencies of this clade and other swine IAV clades in USDA IAV-in-swine data are not a measure of prevalence: these data are derived from the passive sampling of clinically sick pigs (37). Despite this limitation, the surveillance provides a 10-year time series for each genetic clade circulating in U.S. swine, allowing the meaningful identification of changes in detection frequency relative to historical counts. We suggest that a pattern of increasing detection frequency paired with low relative genetic diversity can act as an early warning signal that can be used to flag genetic clades of swine IAV that require characterization and risk assessment for swine agriculture and pandemic preparedness.

To determine whether a selective sweep occurred due to antigenic drift, we identified amino acid substitutions sustained in the major and minor clades that were circulating as the detection frequency increased from 2018 to 2020. We identified an N156H substitution in the HA of the major clade. Amino acid position 156 was previously identified as having an effect on the antigenic phenotype, usually in combination with substitutions in other positions on the HA (11, 15, 38), but the impact of an amino acid substitution depends on the biological properties of the specific amino acid(s) that changed in the context of the overall HA1 amino acid sequence (39, 40). This N156H

substitution prompted the antigenic characterization of the major and minor clades via HI assays to assess for a potential loss in cross-reactivity. A significant loss in cross-reactivity of the contemporary 156H from previous strains with 156N would suggest a potential lack of population immunity that could explain the increased frequency of the major clade. However, our data did not demonstrate that the substitution caused significant antigenic drift. Antibodies raised against ancestral C-IVA demonstrated HI cross-reactivity against the more recent strains regardless of the substitution. Our results support previous findings that variation at position 156 alone did not cause significant antigenic drift (15, 38). The limited change in antigenic phenotype suggests that the N156H substitution may not have been the primary cause of the observed clonal expansion of the C-IVA major clade.

With no evidence of significant antigenic drift in the HA between the contemporary C-IVA major and minor clades, the viruses were analyzed for evidence of other genetic signatures associated with expansion. The minor clade recently reassorted to acquire N2-2002A.2 genes, while the major clade remained paired with N2-2002B.2. A phylogenetic analysis suggested that the most likely donor of the N2-2002A.2 gene was an H1 beta virus. This H1 genetic clade is not frequently detected, with only 104 detections from January 2011 to March 2021 (see Fig. S1 in the supplemental material). Not all regions of the United States are sampled equally in the passive surveillance program; there can be geographical areas and production systems that are underrepresented (27), and swine and their IAVs may move into the United States from regions with far less surveillance (e.g., see reference 41). Our analysis supports the proposition that infrequently detected clades of IAV can contribute to IAV reassortment and increase genetic diversity, and this may result in novel viruses that have the capacity to expand across the United States (31).

We further investigated the antigenic effects of this reassortment event with a panel of NI antisera previously used to describe antigenic variation among and between swine N2 lineages (30). The 2002B.2 of the C-IVA major clade viruses retained close antigenic relationships with the 2002B.2 reference antigen, but antigenic variation existed between clade representatives within the 2002 lineage. Since the early-emerging 2010.1 viruses were paired with 2002A at the time when they began to outnumber the previously circulating C-IVA viruses, population immunity may have been skewed toward both mismatched HA and NA. The 2002B.2 clade of N2 now represents the majority of circulating N2 detected in the swine population, so the importance of NA immunity for the maintenance of the major C-IVA H3 clade paired with 2002B is not clear.

We analyzed whole-genome sequencing (WGS) data for evidence of reassortment of the internal genes. The major C-IVA clade was determined to have reassorted with other endemic swine viruses, likely an H1 delta1 virus, to acquire an NP of the H1N1pdm09 lineage. The H1 delta1 clade was fairly common from 2011 to 2017, making up 17 to 47% of yearly IAV (H1 and H3) detections (Fig. S1). The phylogenetic analysis also revealed other NP reassortment events in the major clade of C-IVA, suggesting that although the C-IVA NPs all share the same NP pdm evolutionary lineage circulating in swine, they are derived from different donor H1 and H3 swine viruses. The genotype of swine IAV internal genes was summarized as a concatenation of one-letter codes representing the genetic lineage of each gene segment (PB2, PB1, PA, NP, M, and NS) without the HA and NA segments. The C-IVA internal gene constellation in 2010 was TTTTTT, with all internal genes coming from the TRIG lineage. C-IVA viruses then acquired a matrix gene from the H1N1pdm09 virus, with constellation TTTTPT, and this was common between 2009 and 2016 (42). This constellation was also involved in an H3N2v outbreak in humans from 2011 to 2012, causing 340 cases across 13 U.S. states (43). However, beginning in 2017, the internal gene constellation found in the C-IVA major clade that increased in detection frequency was TTTTPT with an H1N1pdm09 NP gene. This constellation was observed previously but was uncommon (22 of the 368 isolates between 2009 and 2016) (42). Influenza NP is characterized as a structural RNA binding protein that forms the ribonucleoprotein (RNP) particle (44), and its genetic variation may impact functions such as the temporal regulation of apoptosis or the import and export of viral RNPs (vRNPs) from the nucleus (45, 46). Results from a transmission study in pigs have demonstrated that H3 viruses with the

TTTTPT constellation are more effective in viral transmission than H3 strains with a TTTTPT constellation (42). Consequently, our data suggest that the success of this clade of viruses could be explained by differences between the pdm09 and TRIG genetic lineages of the NP acquired following reassortment in 2017.

Since H3 C-IVA viruses continue to make up roughly one-half of H3N2 detections within the national USDA influenza A virus-in-swine surveillance program in 2021, the increased detection frequency of C-IVA suggests that vaccines should include antigens from this clade of IAV. Subsequent surveillance is necessary to determine if vaccination against C-IVA will result in a decrease in detection; however, this would require additional knowledge of farm-specific vaccines and vaccination strategies. Matching vaccine components to circulating diversity and understanding how swine transportation patterns and biosecurity practices affect the transmission of swine IAV H3 clades can help improve animal health. Our analysis also demonstrates how low-frequency or regionally restricted genotypes donated gene segments to a different HA clade that subsequently led to the expansion of newly reassorted gene combinations. This dynamic and the resurgence of the H3 C-IVA clade create concern for public health, with the knowledge that a virus from the same clade was involved in causing a human outbreak in the context of reassortment. Our HI assay included a representative strain (A/swine/New York/A01104005/2011) that was genetically similar to the H3N2v from the 2011–2012 outbreaks and showed that the contemporary C-IVA representatives tested had not undergone significant antigenic drift. However, dominant swine H3N2 clades have caused numerous zoonotic events through human-swine agricultural interfaces (43, 47, 48), and more recent contemporary C-IVA swine strains may be antigenically drifted from the pandemic preparedness candidate vaccine virus A/Minnesota/11/2010 (49). Thus, understanding the factors that contribute to IAV in swine clade expansion is necessary to inform and improve prediction methods for more successful control measures and to provide insight into pandemic preparedness efforts.

MATERIALS AND METHODS

Data collection. All available U.S. swine H3 nucleotide sequences ($n = 3,395$) detected between January 2010 and March 2021 deposited in GenBank (50) were downloaded from the Influenza Research Database (IRD) (51). These sequences included all of the USDA swine IAV surveillance data ($n = 2,463$) and publicly shared data from other sources. Duplicate strains were removed from the data set. Sequences were then classified using octoFLU (52), and those that were from the C-IVA clade ($n = 1,376$) were retained for further analysis. All available corresponding NA gene segments ($n = 1,291$) and whole-genome sequences ($n = 545$) were collated and classified into lineages using octoFLU (52) according to the N2-1998 and N2-2002 clade divisions introduced by Kaplan et al. (30). The H3 clade detection frequency was derived from public sequence data and validated with the private regional surveillance data housed in the Iowa State University Veterinary Diagnostic Lab (ISU VDL), visualized on ISU FLUture (23).

Estimation of relative genetic diversity. To generate a computationally tractable data set, we generated a random subset ($n = 500$) of H3 C-IVA sequences via smof v2.21.0 (53). Sequences were aligned with mafft v7.450 (54), and a maximum likelihood phylogenetic tree was inferred using the generalized time-reversible (GTR) model of nucleotide substitution in FastTree v2.1.11 (55). This tree was used in a root-to-tip regression analysis in TempEst v1.5.3 (56) to assess temporal signals and detect genes with incongruous genetic divergence and sampling dates. The final data set ($n = 493$) was then analyzed with BEAST v1.8.4 (57) to estimate the effective population size of the C-IVA lineage over time. We applied the GMRF Bayesian Skyride coalescent model (58) with a GTR substitution model with gamma-distributed rate variation, an uncorrelated relaxed clock, and a Markov chain Monte Carlo (MCMC) chain length of 100,000,000, with sampling every 10,000 iterations. Demographic reconstruction was performed using the GMRF Skyride reconstruction in Tracer v1.7.1 (59), and a maximum clade credibility (MCC) tree was generated using TreeAnnotator v1.8.4 (60). Clades were defined as a monophyletic group with at least 10 detections, circulation across multiple years, and significant statistical support (posterior probability of >70).

Deployment of Nextstrain for H3 IAV in swine. The Nextstrain (28) platform was adapted for H3 IAV in swine. A time-scaled tree was estimated for all H3 swine IAV HA genes and a focused C-IVA HA nucleotide sequence data set using the refine Augur command (61). A separate time-scaled tree was estimated for paired NA nucleotide sequences, and the two trees were then compared using the Auspice visualization platform (<https://github.com/nextstrain/auspice>). Amino acid substitutions were annotated on the backbone of the tree using the ancestral and translate commands. The H3 antigenic motif was visualized by combining the Color by Genotype function for positions 145, 155, 156, 158, 159, and 189. The lineages determined through octoFLU of the other six gene segments were mapped onto the HA tree using the traits command. The traits command also integrated geographic information at the U.S. state level and computed putative transmission between states. These data were exported as JSON files

that are interactively visualized on the Web at <https://flu-crew.org/> on an AWS server using USDA-ARS SCInet, with all files provided at <https://github.com/flu-crew/h3-iva-evolution>.

Inference of reassortment and ancestral states of H3 C-IVA. We generated two additional sequence data sets to identify the likely origin of the NP and N2-2002A gene segments paired with the C-IVA HA genes following reassortment. All N2-2002A sequences paired with H1 or H3 from January 2011 to March 2021 ($n = 191$) were downloaded and classified using octoFLU. The previously collected C-IVA NP genes were merged with NP genes from commonly detected swine clades during the same time frame with the whole-genome constellation TTTTPT (H1 delta1a, delta1b, delta2, and gamma and H3 2010.1) ($n = 159$) alongside a set of randomly selected human pdm NP genes from influenza seasons spanning 2009 through 2018 to 2019 ($n = 73$). Strain names were used to match the downloaded NA and NP genes with the corresponding clade of the HA gene of the sequenced virus. If mixed infections were detected, strains were included once for each HA sequenced from the sample. Subsequently, we inferred the HA ancestral state across the NA and NP gene trees to identify the donor of the pdm NP and NA 2002A genes using a migration model in TreeTime v0.8.6 (62) with default settings. Annotated trees were visualized using FigTree v1.4.4 (63).

Antigenic characterization. We identified two C-IVA genetic clades cocirculating in the United States from January 2019 to March 2021: one clade formed the majority of detections (89.3% of 326 sequences), and the other was minor but persistent. To identify a representative sequence for each clade, we generated an HA1 consensus sequence in Geneious Prime 2020.2.3 and selected the best-matching field strain from the USDA IAV-in-swine surveillance system repository at the National Veterinary Services Laboratories, USDA-APHIS. For the major clade, we identified an amino acid substitution at position 156 on the backbone of the phylogeny using Nextstrain. We selected an “ancestral” strain and a “contemporary” strain to reflect the substitution at position 156. Three field strains most similar to the consensus sequences were selected to be antigenically characterized: A/swine/Oklahoma/A01770191/2015 (OK/15) as the C-IVA major ancestral strain, A/swine/North Carolina/A02245294/2019 (NC/19) as the C-IVA major contemporary strain, and A/swine/Minnesota/A02266068/2018 (MN/18) as the C-IVA minor strain.

A panel of swine antisera was selected using sera previously produced by immunizing two pigs (11, 38). Antisera were treated with receptor-destroying enzyme (II) (Hardy Diagnostics), heat inactivated at 56°C for 30 min, and adsorbed with 50% turkey red blood cells to remove nonspecific hemagglutination inhibitors. Hemagglutination inhibition (HI) assays were performed on test antigens and selected sera using turkey red blood cells (64). Cross-HI tables were merged and mapped in 3 dimensions according to an established antigenic cartography method (11). Antigenic distances between viruses were calculated in antigenic units (AU), in which 1 AU is equivalent to a 2-fold loss in HI cross-reactivity. A threshold of ≥ 3 AU is considered a significant loss in cross-reactivity (11). HI data with the selected H3 C-IVA strains were merged with a subset of previously generated H3 antigenic data and used to create three-dimensional (3-D) antigenic maps using antigenic cartography (9, 11, 38). Antigenic distances between antigens generated in the 3-D map were extracted and plotted using ggplot2 in R (65).

An enzyme-linked lectin assay (ELLA) was used to determine neuraminidase-inhibiting (NI) antibody titers. Serial dilutions of swine neuraminidase antisera were incubated with standardized concentrations of IAV in fetuin-coated 96-well plates for 16 h at 37°C with 5% CO₂. Cleavage of sialic acids from fetuin was detected using peanut agglutinin-horseradish peroxidase (PNA-HRP) (Sigma-Aldrich, St. Louis, MO) and 3,3',5,5'-tetramethylbenzidine (TMB) (KPL Laboratories, Gaithersburg, MD), as previously described (66, 67). The optical density (OD) of the plates was read at 650 nm, and the titer was assigned as the reciprocal of the highest dilution resulting in at least 50% inhibition.

Data availability. All sequence data are publicly available in NCBI GenBank, and the code, data, and supplemental material associated with this study are provided at <https://github.com/flu-crew/h3-iva-evolution>. Nextstrain for H3 swine IAV is hosted at <https://flu-crew.org/>.

SUPPLEMENTAL MATERIAL

Supplemental material is available online only.

FIG S1, PDF file, 0.2 MB.

FIG S2, PDF file, 0.3 MB.

FIG S3, PDF file, 0.1 MB.

FIG S4, PDF file, 0.2 MB.

TABLE S1, PDF file, 0.1 MB.

TABLE S2, PDF file, 0.1 MB.

ACKNOWLEDGMENTS

We gratefully acknowledge pork producers, swine veterinarians, and laboratories for participating in the USDA influenza A virus-in-swine surveillance system and publicly sharing sequences.

This work was supported in part by the Iowa State University Presidential Interdisciplinary Research Initiative; the Iowa State University Veterinary Diagnostic Laboratory; the U.S. Department of Agriculture (USDA) Agricultural Research Service (ARS) (project number 5030-32000-231-000-D); the National Institute of Allergy and Infectious

Diseases, National Institutes of Health, Department of Health and Human Services (contract number 75N93021C00015); the USDA Agricultural Research Service Research Participation Program of the Oak Ridge Institute for Science and Education (ORISE) through an interagency agreement between the U.S. Department of Energy (DOE) and the USDA Agricultural Research Service (contract number DE-AC05-06OR23100); the Department of Defense, Defense Advanced Research Projects Agency, Preventing Emerging Pathogenic Threats program (contract number HR00112020034); and the SCLnet project of the USDA-ARS (project number 0500-00093-001-00-D). The funders had no role in study design, data collection and interpretation, or the decision to submit the work for publication. Mention of trade names or commercial products in this article is solely for the purpose of providing specific information and does not imply recommendation or endorsement by the USDA, DOE, ORISE, DARPA, or ISU. The USDA is an equal opportunity provider and employer.

REFERENCES

- Muramoto Y, Noda T, Kawakami E, Akkina R, Kawaoka Y. 2013. Identification of novel influenza A virus proteins translated from PA mRNA. *J Virol* 87:2455–2462. <https://doi.org/10.1128/JVI.02656-12>.
- Yamayoshi S, Watanabe M, Goto H, Kawaoka Y. 2016. Identification of a novel viral protein expressed from the PB2 segment of influenza A virus. *J Virol* 90:444–456. <https://doi.org/10.1128/JVI.02175-15>.
- Gamblin SJ, Skehel JJ. 2010. Influenza hemagglutinin and neuraminidase membrane glycoproteins. *J Biol Chem* 285:28403–28409. <https://doi.org/10.1074/jbc.R110.129809>.
- Essere B, Yver M, Gavazzi C, Terrier O, Isel C, Fournier E, Giroux F, Textoris J, Julien T, Socratous C, Rosa-Calatrava M, Lina B, Marquet R, Moules V. 2013. Critical role of segment-specific packaging signals in genetic reassortment of influenza A viruses. *Proc Natl Acad Sci U S A* 110:E3840–E3848. <https://doi.org/10.1073/pnas.1308649110>.
- Marshall N, Priyamvada L, Ende Z, Steel J, Lowen AC. 2013. Influenza virus reassortment occurs with high frequency in the absence of segment mismatch. *PLoS Pathog* 9:e1003421. <https://doi.org/10.1371/journal.ppat.1003421>.
- Te Velthuis AJW, Fodor E. 2016. Influenza virus RNA polymerase: insights into the mechanisms of viral RNA synthesis. *Nat Rev Microbiol* 14: 479–493. <https://doi.org/10.1038/nrmicro.2016.87>.
- Nicholls JM, Chan RW, Russell RJ, Air GM, Peiris JS. 2008. Evolving complexities of influenza virus and its receptors. *Trends Microbiol* 16:149–157. <https://doi.org/10.1016/j.tim.2008.01.008>.
- Ito T, Couceiro JN, Kelm S, Baum LG, Krauss S, Castrucci MR, Donatelli I, Kida H, Paulson JC, Webster RG, Kawaoka Y. 1998. Molecular basis for the generation in pigs of influenza A viruses with pandemic potential. *J Virol* 72:7367–7373. <https://doi.org/10.1128/JVI.72.9.7367-7373.1998>.
- Smith DJ, Lapedes AS, de Jong JC, Bestebroer TM, Rimmelzwaan GF, Osterhaus ADME, Fouchier RAM. 2004. Mapping the antigenic and genetic evolution of influenza virus. *Science* 305:371–376. <https://doi.org/10.1126/science.1097211>.
- Bedford T, Suchard MA, Lemey P, Dudas G, Gregory V, Hay AJ, McCauley JW, Russell CA, Smith DJ, Rambaut A. 2014. Integrating influenza antigenic dynamics with molecular evolution. *Elife* 3:e01914. <https://doi.org/10.7554/eLife.01914>.
- Lewis NS, Anderson TK, Kitikoon P, Skepner E, Burke DF, Vincent AL. 2014. Substitutions near the hemagglutinin receptor-binding site determine the antigenic evolution of influenza A H3N2 viruses in U.S. swine. *J Virol* 88:4752–4763. <https://doi.org/10.1128/JVI.03805-13>.
- Koel BF, Burke DF, Bestebroer TM, van der Vliet S, Zondag GCM, Vervaeck G, Skepner E, Lewis NS, Spronken MIJ, Russell CA, Eropkin MY, Hurt AC, Barr IG, de Jong JC, Rimmelzwaan GF, Osterhaus ADME, Fouchier RAM, Smith DJ. 2013. Substitutions near the receptor binding site determine major antigenic change during influenza virus evolution. *Science* 342: 976–979. <https://doi.org/10.1126/science.1244730>.
- Santos JJS, Abente EJ, Obadan AO, Thompson AJ, Ferreri L, Geiger G, Gonzalez-Reiche AS, Lewis NS, Burke DF, Rajao DS, Paulson JC, Vincent AL, Perez DR. 2019. Plasticity of amino acid residue 145 near the receptor binding site of H3 swine influenza A viruses and its impact on receptor binding and antibody recognition. *J Virol* 93:e01413-18. <https://doi.org/10.1128/JVI.01413-18>.
- Burke DF, Smith DJ. 2014. A recommended numbering scheme for influenza A HA subtypes. *PLoS One* 9:e112302. <https://doi.org/10.1371/journal.pone.0112302>.
- Abente EJ, Santos J, Lewis NS, Gauger PC, Stratton J, Skepner E, Anderson TK, Rajao DS, Perez DR, Vincent AL. 2016. The molecular determinants of antibody recognition and antigenic drift in the H3 hemagglutinin of swine influenza A virus. *J Virol* 90:8266–8280. <https://doi.org/10.1128/JVI.01002-16>.
- Vincent AL, Perez DR, Rajao D, Anderson TK, Abente EJ, Walia RR, Lewis NS. 2017. Influenza A virus vaccines for swine. *Vet Microbiol* 206:35–44. <https://doi.org/10.1016/j.vetmic.2016.11.026>.
- Loving CL, Lager KM, Vincent AL, Brockmeier SL, Gauger PC, Anderson TK, Kitikoon P, Perez DR, Kehrl ME, Jr. 2013. Efficacy in pigs of inactivated and live attenuated influenza virus vaccines against infection and transmission of an emerging H3N2 similar to the 2011–2012 H3N2v. *J Virol* 87: 9895–9903. <https://doi.org/10.1128/JVI.01038-13>.
- Kitikoon P, Nilubol D, Erickson BJ, Janke BH, Hoover TC, Sornsen SA, Thacker EL. 2006. The immune response and maternal antibody interference to a heterologous H1N1 swine influenza virus infection following vaccination. *Vet Immunol Immunopathol* 112:117–128. <https://doi.org/10.1016/j.vetimm.2006.02.008>.
- Webby RJ, Swenson SL, Krauss SL, Gerrish PJ, Goyal SM, Webster RG. 2000. Evolution of swine H3N2 influenza viruses in the United States. *J Virol* 74:8243–8251. <https://doi.org/10.1128/jvi.74.18.8243-8251.2000>.
- Zhou NN, Senne DA, Landgraf JS, Swenson SL, Erickson G, Rossow K, Liu L, Yoon K, Krauss S, Webster RG. 1999. Genetic reassortment of avian, swine, and human influenza A viruses in American pigs. *J Virol* 73:8851–8856. <https://doi.org/10.1128/JVI.73.10.8851-8856.1999>.
- Anderson TK, Chang J, Arendsee ZW, Venkatesh D, Souza CK, Kimble JB, Lewis NS, Davis CT, Vincent AL. 2021. Swine influenza A viruses and the tangled relationship with humans. *Cold Spring Harb Perspect Med* 11: a038737. <https://doi.org/10.1101/cshperspect.a038737>.
- Kitikoon P, Nelson MI, Killian ML, Anderson TK, Koster L, Culhane MR, Vincent AL. 2013. Genotype patterns of contemporary reassorted H3N2 virus in US swine. *J Gen Virol* 94:1236–1241. <https://doi.org/10.1099/vir.0.51839-0>.
- Zeller MA, Anderson TK, Walia RW, Vincent AL, Gauger PC. 2018. ISU FLU-ture: a veterinary diagnostic laboratory Web-based platform to monitor the temporal genetic patterns of influenza A virus in swine. *BMC Bioinformatics* 19:397. <https://doi.org/10.1186/s12859-018-2408-7>.
- Rajao DS, Gauger PC, Anderson TK, Lewis NS, Abente EJ, Killian ML, Perez DR, Sutton TC, Zhang J, Vincent AL. 2015. Novel reassortant human-like H3N2 and H3N1 influenza A viruses detected in pigs are virulent and antigenically distinct from swine influenza viruses endemic to the United States. *J Virol* 89:11213–11222. <https://doi.org/10.1128/JVI.01675-15>.
- Anderson TK, Nelson MI, Kitikoon P, Swenson SL, Korslund JA, Vincent AL. 2013. Population dynamics of cocirculating swine influenza A viruses in the United States from 2009 to 2012. *Influenza Other Respir Viruses* 7(Suppl 4):42–51. <https://doi.org/10.1111/irv.12193>.
- Arendsee ZW, Chang J, Hufnagel DE, Markin A, Janas-Martindale A, Vincent AL, Anderson TK. 2021. octoFLUshow: an interactive tool describing spatial and temporal trends in the genetic diversity of influenza A virus in U.S. swine. *Microbiol Resour Announc* 10:e01081-21. <https://doi.org/10.1128/MRA.01081-21>.
- Walia RR, Anderson TK, Vincent AL. 2019. Regional patterns of genetic diversity in swine influenza A viruses in the United States from 2010 to 2016. *Influenza Other Respir Viruses* 13:262–273. <https://doi.org/10.1111/irv.12559>.

28. Hadfield J, Megill C, Bell SM, Huddleston J, Potter B, Callender C, Sagulenko P, Bedford T, Neher RA. 2018. Nextstrain: real-time tracking of pathogen evolution. *Bioinformatics* 34:4121–4123. <https://doi.org/10.1093/bioinformatics/bty407>.
29. Bush RM, Bender CA, Subbarao K, Cox NJ, Fitch WM. 1999. Predicting the evolution of human influenza A. *Science* 286:1921–1925. <https://doi.org/10.1126/science.286.5446.1921>.
30. Kaplan BS, Anderson TK, Chang J, Santos J, Perez D, Lewis N, Vincent AL. 2021. Evolution and antigenic advancement of N2 neuraminidase of swine influenza A viruses circulating in the United States following two separate introductions from human seasonal viruses. *J Virol* 95:e00632–21. <https://doi.org/10.1128/JVI.00632-21>.
31. Zeller MA, Chang J, Vincent AL, Gauger PC, Anderson TK. 2021. Spatial and temporal coevolution of N2 neuraminidase and H1 and H3 hemagglutinin genes of influenza A virus in US swine. *Virus Evol* 7:veab090. <https://doi.org/10.1093/ve/veab090>.
32. Jansen ML. 2017. Technical update: updated FluSure XP offers cross-protection in pigs challenged with contemporary cluster IV-A H3N2 swine influenza virus. Zoetis Inc, Parsippany, NJ.
33. Sandbulte MR, Spickler AR, Zaabel PK, Roth JA. 2015. Optimal use of vaccines for control of influenza A virus in swine. *Vaccines (Basel)* 3:22–73. <https://doi.org/10.3390/vaccines3010022>.
34. United States Department of Agriculture. 2016. Swine 2012 part II: reference of swine health and health management in the United States, 2012. US Department of Agriculture, Fort Collins, CO. Accessed 23 April 2022. https://www.aphis.usda.gov/animal_health/nahms/swine/downloads/swine2012/Swine2012_dr_PartII_revised.pdf.
35. Kligen TR, Reimering S, Loers J, Mooren K, Klawonn F, Krey T, Gabriel G, McHardy AC. 2018. Sweep dynamics (SD) plots: computational identification of selective sweeps to monitor the adaptation of influenza A viruses. *Sci Rep* 8:373. <https://doi.org/10.1038/s41598-017-18791-z>.
36. Rambaut A, Pybus OG, Nelson MI, Viboud C, Taubenberger JK, Holmes EC. 2008. The genomic and epidemiological dynamics of human influenza A virus. *Nature* 453:615–619. <https://doi.org/10.1038/nature06945>.
37. Vincent AL, Lager KM, Janke BH, Gramer MR, Richt JA. 2008. Failure of protection and enhanced pneumonia with a US H1N2 swine influenza virus in pigs vaccinated with an inactivated classical swine H1N1 vaccine. *Vet Microbiol* 126:310–323. <https://doi.org/10.1016/j.vetmic.2007.07.011>.
38. Bolton MJ, Abente EJ, Venkatesh D, Stratton JA, Zeller M, Anderson TK, Lewis NS, Vincent AL. 2019. Antigenic evolution of H3N2 influenza A viruses in swine in the United States from 2012 to 2016. *Influenza Other Respir Viruses* 13:83–90. <https://doi.org/10.1111/irv.12610>.
39. Zeller MA, Gauger PC, Arendsee ZW, Souza CK, Vincent AL, Anderson TK. 2021. Machine learning prediction and experimental validation of antigenic drift in H3 influenza A viruses in swine. *mSphere* 6:e00920–20. <https://doi.org/10.1128/mSphere.00920-20>.
40. Sun H, Yang J, Zhang T, Long LP, Jia K, Yang G, Webby RJ, Wan XF. 2013. Using sequence data to infer the antigenicity of influenza virus. *mBio* 4:e00230–13. <https://doi.org/10.1128/mBio.00230-13>.
41. Nelson MI, Culhane MR, Trovao NS, Patnayak DP, Halpin RA, Lin X, Shilts MH, Das SR, Detmer SE. 2017. The emergence and evolution of influenza A (H1alpha) viruses in swine in Canada and the United States. *J Gen Virol* 98:2663–2675. <https://doi.org/10.1099/jgv.0.000924>.
42. Rajao DS, Walia RR, Campbell B, Gauger PC, Janas-Martindale A, Killian ML, Vincent AL. 2017. Reassortment between swine H3N2 and 2009 pandemic H1N1 in the United States resulted in influenza A viruses with diverse genetic constellations with variable virulence in pigs. *J Virol* 91:e01763–16. <https://doi.org/10.1128/JVI.01763-16>.
43. Centers for Disease Control and Prevention. 2012. Influenza A (H3N2) variant virus-related hospitalizations: Ohio, 2012. *MMWR Morb Mortal Wkly Rep* 61:764–767.
44. Pons MW, Schulze IT, Hirst GK, Hauser R. 1969. Isolation and characterization of the ribonucleoprotein of influenza virus. *Virology* 39:250–259. [https://doi.org/10.1016/0042-6822\(69\)90045-2](https://doi.org/10.1016/0042-6822(69)90045-2).
45. Portela A, Digard P. 2002. The influenza virus nucleoprotein: a multifunctional RNA-binding protein pivotal to virus replication. *J Gen Virol* 83:723–734. <https://doi.org/10.1099/0022-1317-83-4-723>.
46. Mayank AK, Sharma S, Nailwal H, Lal SK. 2015. Nucleoprotein of influenza A virus negatively impacts antiapoptotic protein API5 to enhance E2F1-dependent apoptosis and virus replication. *Cell Death Dis* 6:e2018. <https://doi.org/10.1038/cddis.2015.360>.
47. Kitikoon P, Gauger PC, Anderson TK, Culhane MR, Swenson S, Loving CL, Perez DR, Vincent AL. 2013. Swine influenza virus vaccine serologic cross-reactivity to contemporary US swine H3N2 and efficacy in pigs infected with an H3N2 similar to 2011–2012 H3N2v. *Influenza Other Respir Viruses* 7(Suppl 4):32–41. <https://doi.org/10.1111/irv.12189>.
48. Shu B, Garten R, Emery S, Balish A, Cooper L, Sessions W, Deyde V, Smith C, Berman L, Klimov A, Lindstrom S, Xu X. 2012. Genetic analysis and antigenic characterization of swine origin influenza viruses isolated from humans in the United States, 1990–2010. *Virology* 422:151–160. <https://doi.org/10.1016/j.virol.2011.10.016>.
49. Souza CK, Anderson TK, Chang J, Venkatesh D, Lewis NS, Pekosz A, Shaw-Saliba K, Rothman RE, Chen KF, Vincent AL. 2022. Antigenic distance between North American swine and human seasonal H3N2 influenza A viruses as an indication of zoonotic risk to humans. *J Virol* 96:e01374–21. <https://doi.org/10.1128/JVI.01374-21>.
50. Benson DA, Cavanaugh M, Clark K, Karsch-Mizrachi I, Lipman DJ, Ostell J, Sayers EW. 2013. GenBank. *Nucleic Acids Res* 41:D36–D42. <https://doi.org/10.1093/nar/gks1195>.
51. Zhang Y, Aevermann BD, Anderson TK, Burke DF, Dauphin G, Gu Z, He S, Kumar S, Larsen CN, Lee AJ, Li X, Macken C, Mahaffey C, Pickett BE, Reardon B, Smith T, Stewart L, Suloway C, Sun G, Tong L, Vincent AL, Walters B, Zaremba S, Zhao H, Zhou L, Zmasek C, Klem EB, Scheuermann RH. 2017. Influenza Research Database: an integrated bioinformatics resource for influenza virus research. *Nucleic Acids Res* 45:D466–D474. <https://doi.org/10.1093/nar/gkw857>.
52. Chang J, Anderson TK, Zeller MA, Gauger PC, Vincent AL. 2019. octoFLU: automated classification for the evolutionary origin of influenza A virus gene sequences detected in U.S. swine. *Microbiol Resour Announc* 8:e00673–19. <https://doi.org/10.1128/MRA.00673-19>.
53. Arendsee ZW, Chang J, Leung E. 2018. incertae-sedis/smof: first release (version 2.13.1). <https://doi.org/10.5281/zenodo.1434656>.
54. Katoh K, Standley DM. 2013. MAFFT multiple sequence alignment software version 7: improvements in performance and usability. *Mol Biol Evol* 30:772–780. <https://doi.org/10.1093/molbev/mst010>.
55. Price MN, Dehal PS, Arkin AP. 2010. FastTree 2—approximately maximum-likelihood trees for large alignments. *PLoS One* 5:e9490. <https://doi.org/10.1371/journal.pone.0009490>.
56. Rambaut A, Lam TT, Max Carvalho L, Pybus OG. 2016. Exploring the temporal structure of heterochronous sequences using TempEst (formerly Path-O-Gen). *Virus Evol* 2:vew007. <https://doi.org/10.1093/ve/vew007>.
57. Drummond AJ, Rambaut A. 2007. BEAST: Bayesian evolutionary analysis by sampling trees. *BMC Evol Biol* 7:214. <https://doi.org/10.1186/1471-2148-7-214>.
58. Minin VN, Bloomquist EW, Suchard MA. 2008. Smooth skyride through a rough skyline: Bayesian coalescent-based inference of population dynamics. *Mol Biol Evol* 25:1459–1471. <https://doi.org/10.1093/molbev/msn090>.
59. Rambaut A, Drummond AJ, Xie D, Baele G, Suchard MA. 2018. Posterior summarization in Bayesian phylogenetics using Tracer 1.7. *Syst Biol* 67:901–904. <https://doi.org/10.1093/sysbio/syy032>.
60. Rambaut A, Drummond AJ. 2015. TreeAnnotator v1. 8.4. MCMC output analysis.
61. Huddleston J, Hadfield J, Sibley TR, Lee J, Fay K, Ilcisin M, Harkins E, Bedford T, Neher RA, Hodcroft EB. 2021. Augur: a bioinformatics toolkit for phylogenetic analyses of human pathogens. *J Open Source Softw* 6:2906. <https://doi.org/10.21105/joss.02906>.
62. Sagulenko P, Puller V, Neher RA. 2018. TreeTime: maximum-likelihood phylogenetic analysis. *Virus Evol* 4:vex042. <https://doi.org/10.1093/ve/vex042>.
63. Rambaut A. 2018. FigTree, version 1.4.4.
64. Kitikoon P, Gauger PC, Vincent AL. 2014. Hemagglutinin inhibition assay with swine sera. *Methods Mol Biol* 1161:295–301. https://doi.org/10.1007/978-1-4939-0758-8_24.
65. Wickham H. 2016. ggplot2: elegant graphics for data analysis, 2nd ed. Springer, Cham, Switzerland. <https://ggplot2.tidyverse.org>.
66. Gao J, Couzens L, Eichelberger MC. 2016. Measuring influenza neuraminidase inhibition antibody titers by enzyme-linked lectin assay. *J Vis Exp* 2016:e54573. <https://doi.org/10.3791/54573>.
67. Kaplan BS, Vincent AL. 2020. Detection and titration of influenza A virus neuraminidase inhibiting (NAI) antibodies using an enzyme-linked lectin assay (ELLA). *Methods Mol Biol* 2123:335–344. https://doi.org/10.1007/978-1-0716-0346-8_24.